Accepted Manuscript

The deep structure of the Iranian Plateau

K. Motaghi, M. Tatar, K. Priestley, F. Romanelli, C. Doglioni, G.F. Panza

PII: S1342-937X(14)00174-9
DOI: doi: 10.1016/j.gr.2014.04.009
Reference: GR 1258

To appear in: *Gondwana Research*

Received date: 26 October 2013
Revised date: 28 February 2014
Accepted date: 22 April 2014

Please cite this article as: Motaghi, K., Tatar, M., Priestley, K., Romanelli, F., Doglioni, C., Panza, G.F., The deep structure of the Iranian Plateau, *Gondwana Research* (2014), doi: 10.1016/j.gr.2014.04.009

The deep structure of the Iranian Plateau

K. Motaghi[1,2,3], M. Tatar[2], K. Priestley[4], F. Romanelli[3,5], C. Doglioni[6], G.F. Panza[3,5,7]

1 Institute for Advanced Studies in Basic Sciences, 45195-1159 Zanjan, Iran

2 International Institute of Earthquake Engineering and Seismology, 19395-3913 Tehran, Iran

3 Department of Mathematics and Geosciences, University of Trieste, Via Weiss, I-34127 Trieste, Italy

4 Bullard Laboratories, University of Cambridge, UK

5 International Centre for Theoretical Physics – SAND group, I-34151 Trieste, Italy

6 Dipartimento Scienze Terra, Universita` La Sapienza, Roma, Italy

7 Institute of Geophysics, China Earthquake Administration, Beijing, 100080, China

Summary

High resolution structures of the lithosphere-asthenosphere system beneath a seismic profile in Iran are obtained by the simultaneous inversion of data from receiver functions and fundamental mode Rayleigh wave group velocity and validated by modeling Bouguer gravity anomaly data. The seismic data are gathered over a profile extending across Zagros, Sanandaj-Sirjan Zone (SSZ), Urumieh-Dokhtar magmatic arc (UDMA), Central Iran, Alborz-Binalud Mountain ranges and Kopeh Dagh Mountain ranges. The results confirm the presence of crustal roots at the north and south of Iranian Plateau where it meets the Arabian Plate and Eurasia. The high velocity lithosphere of the Arabian Plate gently plunges NNE-ward beneath Central Iran supporting the subduction of the continental lithosphere responsible for the seismicity of the area. The crust and lithosphere are thinner beneath Central Iran, where two low velocity structures are very likely related to magma sources of the UDMA and in east of Iran, around Lut block, where the volcanism shows calcalkaline subduction-related geochemistry. The crustal-lithospheric root to the north of the Iranian Plateau may represent the relict of a previous “cimmeric” subduction zone. Therefore the Iranian lithosphere-asthenosphere system could be the result of the coalescence of two separate subduction zones.

- **Key words:** Iranian Plateau, crust, deep structure, joint inversion, receiver function, surface wave , Bouguer gravity modeling

1- Introduction

The complex features in the Iranian crust, lithospheric mantle and asthenosphere structure result from the Arabia-Eurasia Plates convergence. The SSW-overriding of Eurasia over Arabia during late Mesozoic caused the subduction under Central Iran. Collision occurred between ~35 to 12 Ma ago (e.g., Hessami et al., 2001; Allen and Armstrong, 2008; Mouthereau et al., 2012). This collision is associated with two suture zones in Iran: Zagros mountain range in the south, along Main Zagros Thrust (MZT) Fault (e.g. Kaviani et al. 2007; Paul et al. 2010 and references therein); Kopeh Dagh mountain range in the northeast, along Main Kopeh Dagh Fault, Bakharden-Quchan Fault system as well as river between Alborz-Binalud and Kopeh Dagh Mountan ranges, i.e. Atrak River (ATR, Fig. 1) (e.g. Alavi, 1992, 1996; Howlingworth et al. 2006; Shabanian et al. 2009; Motaghi et el. 2012b) (Fig. 1). The convergence during continent-continent collision caused shortening and thickening beneath both Zagros and Kopeh Dagh mountain ranges and the Iranian Plateau, which is located between these mountains. Paul et al. (2006, 2010) analyzed the data gathered by a network of 66 seismological stations (Zagros profile hereafter) along a profile perpendicular to the tectonic strike of Zagros and calculated P receiver functions (PRF) beneath all stations. They found a ~67 km crustal root north of Zagros Mountain, beneath Sanandaj-Sirjan Zone (SSZ, Fig. 1) which is a highly deformed and moderately metamorphosed remnant of the southern margin of Central Iran. Later, Motaghi et al. (2012a) used 16 broadband stations installed along the profile across Central Iran, Binalud and Kopeh Dagh Mountains (NE Iran profile) to do the same analysis. In fact, NE Iran profile (operating from 2006 to 2008) is a continuation of Zagros profile (operating from 2000 to 2001). The later profile overlaps with the older one (with two stations located in similar locations) and follows a similar trend. Motaghi et al (2012a) calculated PRFs and found a ~55 km crustal root beneath Binalud foreland. None of these roots are located beneath high topography, in the study area, thus it is reasonable to speculate that they are supported by relatively deep geodynamic processes and not by the surface load of mountain ranges and the mechanism of isostasy. These studies indicate that the lithospheres of the Arabia and Eurasia Plates along the suture zones are

under-thrust beneath Central Iran and that doubling of lithosphere occurs at the north and south boundaries of Central Iran. Therefore we test whether the presence of two ophiolitic suture zones is indicative of two subduction processes or is the result of an intermediate lithospheric stretching.

Regional tomography studies over Iran show that the low velocity lithosphere of Central Iran is located between two high velocity and probably colder lithospheres of Arabia (e.g. Maggi and Priestley 2005; Kaviani et al. 2007; Shomali et al. 2011; Shad Manamen et al., 2011) and Eurasia (e.g. Motaghi 2012b) Plates. The large amount of crustal seismic activity in the Zagros, Alborz-Binalud and Kopeh Dagh Mountains shows that these ranges are still active (e.g., Maggi et al., 2000; Tatar et al., 2004). Crustal seismicity is observed everywhere in these mountains, but no relevant subcrustal earthquakes have been located, so far (Turkelli et al., 2003). Subduction of continental lithosphere has been demonstrated in the Alps (Panza and Müller, 1978; Panza et al., 1982; Müller and Panza, 1986) and since these pioneering papers has been recognized in several other collisional belts such as the Himalaya or in retreating slabs as in the Apennines (Doglioni et al., 2007). Moreover, the rheology of the continental lithosphere is responsible for the termination of seismicity at a depth less than that of oceanic lithosphere (Carminati et al., 2002). As an example, the Himalayas and central-northern Apennines subduction zones have no deep seismicity, but they are active as shown by any type of geodynamic data. Therefore, the absence of deep seismicity is not an indication of an inactive subduction, which could rather be of continental nature. During collisional stages, the convergence/shortening ratio along subduction zones decreases, due to the increasing partitioning between contraction in the orogenic prism and subduction (Doglioni et al., 2007). Priestley et al. (2012) show a high velocity thickened lithosphere beneath the Zagros which is stabilized from delamination by depletion. The signature for depletion is the volcanic eruptions above the Zagros which have a low density, depleted source (McKenzie and Priestley, unpublished results). These studies show that there are still open questions about the fate of subduction activity beneath the Zagros, although there are several lines of evidences supporting a seismically silent (but active) slab at depth (Chen and Yang, 2004).

About half of the current convergence between Arabia and Eurasia inside Iran (~10 mm/y) is accommodated by shortening in the Zagros Mountains (Tatar et al., 2002) and the remnant is

mainly accommodated across Alborz-Binalud and Kopeh Dagh Mountains as well as South Caspian Sea (Vernant et al., 2004). Both the Eurasia and Arabia Plates move westerly relative to the mantle, albeit Eurasia is faster and overriding SW-ward Arabia (Crespi et al., 2007). This geodynamic framework constrains the active subduction zone, although continental in composition. The relative convergence between the Eurasia and Arabia is complicated by the contemporaneous CCW subrotation (Cuffaro et al., 2008) of the Arabia lower plate. Central Iran consists of a mosaic of various tectonic rigid blocks, the Lut block, located in the east of Iran, is one of these blocks (Fig. 1), and most of the seismic deformation has been concentrated within the deformational zones among these rigid blocks.

The Iranian Plateau is a natural laboratory for investigating geodynamical processes related to the early phases of continent-continent collision. Here we present the high resolution crust and uppermost mantle (lithosphere-asthenosphere system) structure along a transect from the Zagros, which is the north edge of Arabian Plate in south Iran, across Sanandaj-Sirjan metamorphic zone (SSZ), which is a remnant of the southern active margin of Central Iran, Urumieh–Dokhtar magmatic arc (UDMA), which is characterized by volcanic activity from Eocene to Miocene (e.g.Chiu et al., 2013), Central Iran, which is a relatively less deformed block surrounded by active margins, the Alborz-Binalud Mountains which is the north edge of Central Iran to Kopeh Dagh Mountains which is the south edge of Eurasian Turan Plate (Fig. 1). In this paper, we consider the data gathered by broad-band stations of Zagros profile and NE Iran profile to calculate 1-D absolute S-wave velocity distribution with depth beneath each seismic station, using the joint inversion of PRF and Rayleigh-wave dispersion (Julia et al., 2000). To achieve this, we calculate and analyse the PRFs of those records for which the signal to noise ratio can be improved by stacking many waveform traces and we present one or two high quality stacked receiver functions for each station. The procedure used to simultaneously invert the PRF and the surface wave dispersion (Section 4) can be summarized as follows. We juxtapose all absolute 1-D velocity models obtained from the joint inversion to construct a 2-D S-wave velocity model along the profile AB in Fig. 1. The obtained resolution of the lateral variability of the lithosphere-asthenosphere system is validated with the Bouguer gravity anomaly along the profile: starting from a density model obtained from the S-wave velocity model, via a standard relation between density and S-wave velocity (e.g. Ludwig et al., 1970). The density distribution

beneath seismic profile is determined by linear inversion of Bouguer anomaly. The structures resolved by this procedure are interpreted in terms of subduction and asthenosphere upwelling.

2- Data set

From August 2006 to February 2008, the International Institute of Earthquake Engineering and Seismology (IIEES), Tehran, in collaboration with Cambridge University in the United Kingdom installed a temporary network of 16 broadband stations positioned along a profile from the southern edge of Central Iran, across Binalud Mountans to the Kopeh Dagh (inverted triangles in Fig. 1). The profile is oriented N46^{o}E, almost perpendicular to the structural trend of the Binalud and Kopeh Dagh and along the trend of the Tectonic Equator (TE) and its perturbation (Crespi et al., 2007; Panza et al., 2010). Each seismograph consists of a CMG-3TD 120 sec three-component Guralp sensor and CMG-DM24 data loggers belong to Cambridge University. The data were continuously sampled at 100 samples per second and stamped with GPS time.

The interstation distance varies between 20 km and 100 km with an averages ~30 km. The interstation distance is smaller (~20 km) than average in the NE continental collision zones, i.e., Kopeh Dagh and Binalud Mountain ranges, where strong lateral variation in the crustal thickness are expected, and is larger (~50-100 km) in Central Iran which is a less deformed tectonic block. The limited number of seismic instruments and the different logistic situation of Central Iran which can be extremely hot and sandy made it difficult to finding the suitable station location in this area and resulting in larger interstation distance there.

To expand our study area, we used data from Zagros profile (Paul et al., 2006), primarily using the data from the medium and broad-band stations. The average interstation distance of selected stations of this profile was ~35 km. The profile resulting from the merging of Zagros and NE Iran profiles, referred to as the Iran Profile, is 1200 km long and it includes 32 seismic stations (Fig. 1).

We use 250 teleseismic records of earthquakes with magnitude 5.5 or greater and epicentral distances between 25° and 95° (Fig. 2). Around 85% of these events are recorded from back-azimuth of 25^{o} to 125^{o}. Most of the events are in the 40^{o} to 90^{o} distance range.

3- Data Preparation

3-1- Calculation of P-wave Receiver Function (PRF)

For each event, a 120 s time-window centered at the direct P arrival is selected and used for the calculation of the PRF. Receiver functions are determined using the iterative deconvolution method of Ligorria and Ammon (1999). The Gaussian smoothing factor of 1.0 is equivalent of the application of a 0.5 Hz low pass filter to the seismograms. The dataset of acceptable receiver functions were arranged with increasing theoretical back-azimuth. The PRFs calculated for stations located in a less deformed tectonic area, i.e. Central Iran, show a rather simple structure compared with those obtained from stations that are located over the mountain ranges. Some examples of the calculated PRFs are given by Motaghi et al. (2012a).

We next stack the PRFs to improve the signal to noise ratio. Stacking is straightforward when the PRFs are similar to each other and represent the same structure. The PRFs obtained for one station can change with the variation of two parameters: 1- source-station distance, 2- back-azimuth. To overcome the effect of distance on PRFs, we make a move-out correction using a simple migration technique. The basic concept is to apply a time stretching factor and amplitude scale factor to a receiver function to map it into a receiver function generated with a reference ray parameter. To consider the dependence on the back-azimuth, which is due to complicated crustal structure beneath the receiver, we group receiver function with similar P-wave delay time and stack each group separately. The individual PRFs are aligned according to the P-wave arrival and stacked and then used in the modelling of velocity structures using the joint inversion procedure.

3-2- Dispersion data

The data of the fundamental mode Rayleigh-wave group velocities are extracted from the tomographic study by Rahimi et al. (2014). Group velocities from teleseismic events recorded at 29 permanent broad-band stations distributed coverings Iran were measured for the fundamental mode Rayleigh waves, for the 10–100 sec period range. The fundamental mode were identified using the frequency time analysis (FTAN) approach (Levshin et al., 1972; 1992) applied for 1586 teleseismic records. The ray paths were selected in a way to satisfy the two-station method

conditions (e.g., Mitchell, 1995) and the inter-station path average group velocity was calculated using Wiener deconvolution (e.g., Hwang and Mitchell, 1986). More than 240 inter-station group velocity dispersion curves, covering all Iran Plateau, were inverted to prepare tomographic maps by applying the 2-D tomography method described by Yanovskaya and Ditmar (1990). The tests presented by Rahimi et al. (2014) show that resolution length (the mean size of the averaging area) of the tomographic maps is mainly less than 100 km along the Iran profile. The available dispersion data in the region are discretized using a uniform $0.5^{o}\times0.5^{o}$ grid, therefore, in the joint inversion, for each station the fundamental mode Rayleigh wave dispersion is taken from the relevant tomographic $0.5^{o}\times0.5^{o}$ cell containing that station.

4- Inversion procedure

We briefly describe here the procedure we used to jointly invert the stacked receiver function and surface wave dispersion data. We employ the program *joint96* which is available in the software package "Computer Program in Seismology" (Herrmann and Ammon, 2003).

The damped least square method (Menke, 1989) is used to invert the two data sets for a S-wave velocity model. This method is a common regularization method, which searches for the "simplest" model that fits the data within the limits of its variance (Menke, 1989; Ammon et al. 1990). One important parameter in this method, the damping factor that balances the trade-off between model stability and resolution, has been chosen equal to 0.5. The selection of a common value for all the stations may allow some trivial features to enter in the model; however, the stability tests performed after the inversion helped to remove those features successfully.

Another important factor in the joint inversion is the factor, p, that is related to the weight given to the dispersion data in comparison with receiver function. Selecting a high value for p (close to 1) causes more weight to dispersion data in inversion. We select p=0.25 to give more weight to receiver function and find a relatively high resolution model for our study area.

The procedure used for the joint inversion is based on the linearization of a non-linear inversion problem. Based on this fact, the final model is dependent on the initial model. The drawbacks intrinsic in such problems can be minimized by considering reliable starting models obtained from other studies. The initial models used in this study are taken from Rahimi et al. (2014) who has presented a set of S-wave velocity models for each tectonic area of Iran

considered in this study (e.g. Zagros, Central Iran, and Kopeh Dagh), obtained by the Hedgehog inversion of the dispersion curves (e.g. Panza, 1981). Since this method of inversion is nonlinear, it can take into account the non-uniqueness of the inverse problem presenting several models for each region, with an indication of their related uncertainties.

For each initial model, the linearized joint inversion is controlled by a misfit function that controls the variation of percent of fit between the theoretical and experimental receiver functions at each iteration: if the variation is less than %0.05, the process is terminated.

In such a way, we obtain a set of initial models and thus a large set of solutions for each station. It is useful to identify a representative model to summarize and interpret the results. In this study, the representative model is chosen according to the following criteria: the solution with the closest percentage of fit to the average value of all percentage of fits obtained from all the solutions for the station. This criterion reduces the effects of the projection of possible systematic errors into the inverted structural model. This criterion is similar to the selection of the median model.

5- Stability tests

We perform stability tests for each station to find the most robust velocity model that is consistent, within errors, with the observed data sets. The stability tests are made in two steps: 1- search for the "optimal" parameterization for the joint inversion, 2- regularization of the models output of the inversion procedure. The second stability test aims also to investigate if the resolution improvement is localized either in the crust or in the entire model. To answer this question, we divide the layers of the crust and upper mantle by IS/1.5 and IS/1.0 respectively (IS, or "incremental step", is the minimum thickness resolvable by the dispersion data), and compare the resultant models with those in which all layers are divided by IS/1.5. We observe that only in rare cases is the fit improved by the thinning of layers in the upper mantle.

5-1- Search of the "optimal" parameterization

In order to find the optimal parameterization for the joint inversion, we assign to each layer of the model a thickness equal to the IS used in the non-linear inversion of dispersion measurements reported by Rahimi et al. (2014). The IS is dependent on several parameters, including the dispersion curve error (e.g. Panza 1981). Based on the fact that receiver functions are relatively higher frequency time series, they may resolve smaller features in the Earth in comparison with dispersion data. Thus, the layers of the initial models are subdivided in sub-layers with thickness equal to IS divided by 1.0, 1.25, 1.50 and 2.0. We then operate the joint inversion for each parameterization and keep track of the percentage of fit to observed receiver function. If thinning the layers improves the fit, the new parameterization is accepted and a new iteration in the inversion is performed selecting thinner layers. If the improvement is less than 1% (which is chosen empirically), the new parameterization is rejected and the iterations are terminated.

The final models obtained for the four parameterizations, IS/1.0, IS/1.25, IS/1.5, IS/2.0 respectively, are presented in Figure 3 for KAM station. In most of the cases, the procedure of thinning of layers improves the fit to the receiver function up to IS/1.5.

5-2- Regularization of the inverted models

The S-wave velocity model obtained with the receiver function and dispersion data inversion is simplified to one with a smaller number of layers (model regularization). The model regularization permits identifying robust, reliable features of the models (e.g. Foulger et al., 2013) and can be summarized as follows.

The main velocity boundaries in the model are identified and then the average velocity of the layers located between those assumed boundaries is calculated. With this regularized model, by forward modelling, the synthetic receiver function and dispersion curve are computed. If the synthetic curves generally fall within the experimental error bars, the simplified model is considered the end model. Otherwise, smaller features, averaged before, are added again to the simplified model to achieve a better fit (synthetic data within the error bars). This method robustly removes the small structural details that are not really required by the observed data. Figure 4 shows the final model obtained from inversion (blue model in Fig. 4-c) for the station

CHA and the simplified model (red model in Fig. 4-c) as well as synthetic and observed PRFs and dispersion curves. The resolution kernels are computed for the initial crustal structure used on the joint inversion of dispersion curves and receiver functions. For all the stations the model resolution kernels seem reasonable, indicating that the velocity and thickness of the layers are well constraint. Figure 5 represents the resolution kernels calculated for the final velocity model of station CHA, shown in Fig. 4-c. Red lines represent normalized values of each column of the resolution matrix. This matrix is ideally an identity matrix if all inverted parameters are not correlated; in practice, due to the unavoidable correlation, if the model is satisfactorily resolved, it is a matrix with narrow peaks occurring near the main diagonal. This matrix shows that the estimated model parameters turn out to be linear combinations of the correlated true model parameters (Menke 1989). For example, as can be deduced from Fig. 5, the estimated value for layer 15 is the average of the true values for that layer and its two adjacent ones (i.e. layers 14 and 16). The same applies to the other 14 overlying layers, and the one below, but not to layers 17-20. Since the longest available period of the group velocity dispersion curve is 100 s, i.e. surface waves sample to depth less than 350 km and the sensitivity kernels (obtained for all stations) show that the resolvable features are not deeper than 250-300 km, we limit our maximum depth of investigation to 300 km.

6- Independent geophysical constraint: gravity modeling

A powerful approach for defining realistic geophysical models is the joint interpretation of different geophysical data, or at least of one specific data set, constrained by the results of other independent geophysical data. In this section, we use the geometry of the velocity models obtained in previous section as *a priori* constraints for the linear inversion of gravity Bouguer anomaly data to density. The 2-D S-wave velocity model is converted to density model, keeping the layer's geometry fixed, to define the initial density model for the study area. It is well known that a range of densities is possible for rocks with a given seismic velocity (Nafe-Drake relation: Ludwig et al., 1970). The empirical relationship between these two parameters is generally used to connect the S-wave velocity with the density, but with some uncertainty. The density anomaly is calculated by subtracting this density model from a reference density model defined as follows:

density of 2.50 g/cm^3 for the upper 20 km, density of 2.70 g/cm^3 for 20-30 km, density of 3.20 g/cm^3 for 30-200 km and density of 3.55 g/cm^3 for 200-300 km of depth.

The initial misfit between predicted and observed Bouguer anomaly is large, therefore the density in each layer has been iteratively modified by choosing the new value in the range defined by the error band of the Nafe-Drake relation: ±0.2 g/cm^3 in the crust (where the density < 3 g/cm^3) and ±0.22 g/cm^3 for upper mantle (where the density > 3.2 g/cm^3). The smallest perturbation step used is 0.05 g/cm^3, well consistent with the resolving power of our data, and the density perturbation is made following the equation:

$$\rho_f = \rho_i \pm n \cdot 0.05 \text{ g/cm}^3$$

where ρ_i is the starting density and ρ_f the final accepted value, n is the number of perturbation steps and 0.05 is our assumed density resolution.

Observed Bouguer anomaly data, used for this research, were extracted from a global gravity model called GIF48 (Ries et al., 2011) and were retrieved from the database of International Center for Global Earth Models (ICGEM).

7- Results and Discussion

The absolute S-wave velocity structure of the lithosphere-asthenosphere system beneath the Iran profile has been resolved by simultaneously inverting data from receiver functions and fundamental mode Rayleigh wave group velocity. The method generates a 1-D absolute S-velocity model beneath each station. The thickness of crust and seismic lithosphere (called lithosphere, hereafter) are extracted from each calculated 1-D velocity model and presented in Table 1. These values are resolvable with the error in the range ±1.5 to ±3.5 km for the crust and about ±15 km for the lithosphere. These uncertainties are defined as ± half of the parameter's step at that depth (i.e., equal half of minimum thickness, found by first stability test described in section 5). The thickness of lithosphere is equivalent to the depth in which a low velocity layer is distinguished in the obtained 1-D velocity models.

Combining the 35 1-D velocity distributions with depth obtained in this research, a 2-D velocity model beneath Iran, along profile AB in Fig.1, has been assembled. The cross-section

beneath this profile is presented in Figure 6 that shows the crustal velocity model, i.e., velocity distributions with depth up to 70 km, and Figure 7 that shows the lithosphere-asthenosphere system, down to about 300 km depth. A Gaussian filter width of 30 km and 100 km was employed to smooth Figures 6 and 7, respectively. The crustal model is shown in a separate figure because the resolving power of our data set in the crust is higher than in the upper mantle. This model (Figs. 6 and 7) shows evidence for strong heterogeneities in the uppermost 300 km beneath the profile.

7-1- Variability in the crustal structure

The crustal velocity structure is presented in Figure 6. The upper crust (including sedimentary and crystalline layers: depth range 0-20 km, Vs 2.5-3.2 km/s) has the lower velocity in the south and north of the profile, i.e., beneath the Zagros (south of profile) as well as the Kopeh Dagh, Binalud and northmost of Central Iran (north of profile). The higher velocity upper crust is located in the middle of the profile beneath SSZ, UDMA and the south and middle of Central Iran. These observations are consistent with geology. The Zagros area is covered by at least 10 km of Cambrian to Miocene sediments (e.g. Stocklin 1974; Stoneley 1981; Hatzfeld et al., 2003) and it is widely accepted that the construction of the Zagros Mountains has occurred in large part by folding and thickening of the sedimentary cover on the leading edge of the Arabian platform (e.g. see Hatzfeld and Molnar, 2010, and the references therein). This is the forebelt of the double verging orogeny. The Kopeh Dagh has 10–17 km thick Mesozoic and Tertiary sediments which were folded during the Oligo-Miocene orogenic movements (Stocklin 1968; Afshar Harb 1979; Lyberis & Manby 1999). Moving toward the interior of the orogeny, from thin-skinned tectonics, the deformation becomes thick-skinned.

The Moho boundary and an interpolated crustal thickness are shown in Figures 6 and 7 by black squares connected by black dashed line, respectively. The crustal thickness is large beneath Zagros (~50 km) and it increases beneath SSZ and UDMA where it reaches its maximum ~59 km. To the north, a smooth decrease is seen at the south and middle of Central Iran, reaching its local minimum at the middle of Central Iran, ~35 km. Motaghi et al. (2012a)

used a migration method described by Zhu and Kanamori (2000) to migrate P-to-S converted waves from the Moho boundary (extracted from stacked PRFs) to the Moho depth and report an even thinner crust ~ 27.5 km. This value is the smallest crustal thickness reported in Iran so far. The crustal thickness, along the profile, increases beneath the north part of Central Iran and Binalud and a local maximum (~ 55 km) at x ~ 550 km, is seen beneath the Binalud foreland (Fig. 6). The thickness gradually decreases to a minimum beneath Kopeh Dagh Mountains (~ 30 km) where the surface topography reaches values as high as 3000 m. The relatively shallow Moho beneath the Kopeh Dagh, Binalud and Zagros Mountains suggests that these regions are not isostatically supported by a crustal root, but by somewhat deeper process. The variation of Moho depth is not coherent with the variation of topography; instead, the deepest Moho boundary (crustal root) is located under SSZ, UDMA and Binalud foreland (Fig 6). The resolved intra-crustal discontinuities beside crustal roots beneath SSZ and UDMA (Paul et al., 2010) and Binalud foreland (Motaghi et al., 2012b) imply that under-thrusting of Arabian Plate in the south and over-thrusting of Turan Plate in the north respect to Central Iran are responsible for these thickenings. A schematic picture of this crustal doubling is shown in Figure 9. Other details of this figure are discussed in the next sections.

7-2- Variability in the lithosphere-asthenosphere system

Figure 7 represents the absolute S-wave velocity structure along the profile AB (Fig. 1) down to 300 km depth, the maximum penetration depth of our data set. The depth resolution of the data set is determined by the partial derivatives (Urban et al., 1993) of the dispersion curves of the Rayleigh wave fundamental mode with respect to the shear wave velocity at different periods (Rahimi et al., 2014). The lithosphere thickness is marked in Figure 7 by white squares. These squares show the depth in which a low velocity layer is distinguished in the obtained 1-D velocity models based on joint inversion of the PRFs and surface waves dispersion data (for instance see Fig. 3, depth ~ 120 km). The lithosphere thickness beneath Central Iran is roughly constant and mainly varies around 130±15 km. However, beneath other tectonic areas, the lithosphere-asthenosphere boundary is not observable in most cases. Thus, we conclude that there is a thick lithosphere beneath Zagros as well as Binalud and Kopeh Dagh mountain ranges at least thicker than 200 km for Kopeh Dagh and Binalud and thicker than 240 km for Zagros.

These limits for lithosphere thickness obtained from maximum depth in which we have sufficient resolution to resolve low velocity the asthenosphere (Rahimi et al., 2014). The obtained values for lithosphere thickness are in agreement with the values reported by Priestley et al. (2012) for Middle East. Using a large, multimode surface wave data set, they found a high velocity, thick lithosphere extending to ~225 km depth beneath the Zagros, and a low velocity, thin lithosphere (~120 km depth) beneath the central Iran. They did not observe any thickening of the lithosphere beneath NE of Iran.

Recent S receiver function (SRFs) study of Mohammadi et al. (2013a) suggests a 200 km thick lithosphere beneath the Zagros collision zone, and a thin lithosphere, 80-90 km thick, beneath Central Iran and Alborz representing the Arabian and Iranian lithosphere respectively. They interpreted their inclined observed structure within the Arabian lithosphere (at 80-150 km depth) as the remnant of the subducted Neo-Tethyan ocean slab. However, their observations for the remnant of the Neo-Tethyan ocean slab are not supported with our findings. In previous SRFs study (Mohammadi et al., 2013b) a thick lithosphere of about 130 and 150 km had been defined beneath the Zagros and SSZ respectively.

At shallow depths up to ~70 km, the uppermost mantle beneath the whole profile from A to B is slow, but at deeper parts a high speed S-wave velocity upper mantle is observed beneath the Zagros, which persists to more than ~240 km depth. However, the upper mantle beneath the rest of the profile, i.e. central and NE Iran, is slow up to 180 km depth. These results are consistent with observations of Priestley et al., (2012) for upper mantle velocity model of the Middle East derived from the surface wave analysis.

Before interpreting velocity variation in upper mantle, we validated, in section 6 anomalous values against Bouguer gravity anomaly. Figure 8 represents the density model (Fig. 8-lower panel), which predicts Bouguer gravity anomaly (red circles) similar to observed (gray squares) data (Fig. 8-upper panel). Strong heterogeneity along the profile still persists at depths between 60 and 240 km. A high velocity/density lithosphere beneath Zagros (Vs~4.8 km/s, $\rho \geq$ 3.4) is observed plunging beneath SSZ, UDMA and Central Iran. We believe this is the leading edge of Arabian shield subducted under Central Iran. The V-shaped low velocity anomaly just beneath the MZT (area shown by light green at ~ x = -300 km) is confirmed by gravity

modelling: the low density feature in the range 3.0 g/cm^3 and 3.2 g/cm^3 beneath MZT. The effect of this low density anomaly is responsible for the long wavelength negative Bouguer anomaly peaking in this location. Paul et al. (2006) who modelled this anomaly as due to the crustal thickness properties beneath SSZ and UDMA (Fig. 6) proposed a shallow origin for this feature and explained the space shift between Bouguer anomaly and thickened crust introducing a complicated crustal model that implies crustal doubling in the region. We think that a deeper feature, located in upper mantle and thus well consistent with the S-wave velocity model, likely generate such a long wavelength (λ) variation (where $\lambda/2 \sim 600$ km) in the Bouguer anomaly. This V-shaped anomaly provides evidence for a thickened collided lithosphere located beneath the Zagros; the lithospheric upper mantle may not be a single layer feature but instead is a layered feature. Shortening and thickening due to continental collision, (which makes the lithosphere thicker) affect all intra-lithosphere layers. Since we cannot resolve the lower boundary of the lithosphere beneath Zagros, we present this feature as an evidence for thickening of lithosphere and consequent interruption of asthenosphere. In addition, the V-shaped low density feature certainly causes positive buoyancy as it is laterally surrounded by denser material and can contribute to the uplift in Zagros starting from 15-12 Ma and continuing to the present (Mouthereau et al., 2012 and references therein). However, since the Zagros is an on-going continental subduction system, the orogenic uplift can be inferred as related to the shortening and thickening by thrusts and folds of the upper and lower plates, although the belt has not yet reached the topographic and isostatic steady state regime.

Two localized low density/velocity anomalies are seen in front of the V-shaped feature beneath the south and middle of Central Iran at -100 km < x < 100 km and 200 km < x < 400 km at depth between 120 km and 180 km (Fig. 8). These anomalous features are located beneath the thin lithosphere (~135 km) in the study area. The first anomaly is located north of the UDMA, which is a volcanic arc near and sub-parallel to Main Zagros Thrust Fault (MZT) and the suture between Arabian Plate and Central Iran. The second anomaly is located, in Central Iran, beneath stations located at NW of Lut block. The surficial projection of these anomalies are coincide with volcanic extrusions that might be supplied by such low velocity/density features. The feature almost beneath UDMA is probably a partial melting zone due to fluids produced by dehydration of subducted Arabian slab material beneath Central Iran. The inefficient Sn propagation for paths crossing northern and central Iran (Kadinsky-Cade et al., 1981; Sandvol et al., 2001; Al-Damegh

et al., 2004) where our results (Figs. 7 and 8) and the surface tomography model (Priestley et al., 2012) show very slow upper mantle shear wave velocity implies high temperatures and the possible presence of some melt in the uppermost mantle (Molnar and Oliver, 1969). Priestley et al., (2012) using a T(Vs, Z) relation similar to that of Priestley and McKenzie (2006) showed the upper mantle beneath the central Iran has temperature greater than 1405 ±20ºC at 125 km depth. They observed very low temperature at this depth beneath the Zagros.

Above the anomaly in Central Iran in the upper-mantle there are two other interesting features: 1- a low velocity anomaly is located just beneath the crust (around x ~ 300 km, Fig. 7). This feature is confirmed by our density modeling (Fig. 8) and by other investigations on Pn velocity variations beneath the Iranian Plateau (Amini et al. 2012) and we interpret this anomaly as a signature of the accumulation of partial melts at the base of the crust, i.e., underplating; 2- there is a high velocity feature, with two maxima at x ~ 200 km and x ~ 300 km inside the crust (Fig. 6), above the underplating zone and we interpret this high velocity anomaly as a remnant of igneous intrusion into the lower crust.

Some magmatism of the Lut block (46-25 Ma) is calcalkaline-shoshonitic, i.e., constraining the Eocene-Oligocene age and location of the Arabia subduction, when the subduction plane was located more to the NE than now, as expected in a laterally growing belt associated to a NE-directed subduction zones.

Pang et al. (2012) studied the volcanic extrusions positioned around Lut block (Fig. 1). Using 40Ar/39Ar dating they found that volcanism around Lut block occurred from ~14 Ma to 1.6 Ma ago and has a very young origin and that the alkali basalts observed around Lut most likely have asthenospheric origin. The modeling of rare earth elements concentrations in the basalts suggests that the basalts could have been formed by low degrees of partial melting (~3–10%) of an enriched mantle source at garnet-stable depths. Magmas erupted in this setting are geochemically similar to ocean island basalts and there are no geochemical features pointing to arc-related signatures characteristic of the Iranian sub-continental lithospheric mantle (Walker et al. 2009; Pang et al. 2012). However, Mazhari and Safari (2013) have alternatively shown that the volcanism around the Lut block is calcoalkaline. Moreover the Zouzan pluton is one of the intrusive bodies in the NE of Lut block enclosed by Cenozoic volcanic and sedimentary rocks. It

consists of two distinct mafic and felsic magmas which are genetically unrelated. All studied rocks are calc-alkaline in nature, with LILE/REE and HFSE/REE ratios compatible with arc related magmatism (Mazhari and Safari, 2013). Relatively high contents of incompatible elements, low Na2O and Mg#>44 suggest they were derived from partial melting of metabasalt sources in a subduction setting (Mazhari and Safari, 2013). Therefore all this magmatism appear to be formed by partial melting in the mantle wedge in the hanging wall of the Arabian slab beneath Iran.

Our results are compatible with earlier studies - surface wave dispersion (e.g., Kaviani et al., 2007; Maggi and Priestley, 2005, Priestley et al., 2012), Pn velocities (Al-Lazki et al., 2003, 2004; Amini et al., 2012) and P- and S-wave tomography (Alinaghi et al., 2007; Kaviani et al., 2007; Paul et al., 2010) - that found low velocities in the uppermost mantle of Central Iran. But, our findings do not support the idea of a breakoff of the oceanic Neo-Tethyan slab beneath Central Iran as suggested by Mohammadi et al. (2013a) and Shomali et al (2011). A sketch representing a new model for the deep structures beneath Iranian Plateau based on our results is presented in Fig. 9. The geological map, the distribution of separated ophiolite belts, and the migration and widening in time of the orogenic shortening support the notion of at least two independent subduction events since the Mesozoic. This could be associated to the coalescence of microplates intervening between the Eurasian and Arabian plates. NE-directed subduction zones like the Zagros are characterized by slab hinge migrating toward the upper plate. This implies diffuse contraction and double verging orogen in the hangin wall of the subduction zone, plus crustal and lithospheric thickening. Oceanic subduction is superimposed by continental subduction. The double subduction evolution recorded in the surface geology is supported by the geophysical data presented here. The two gravity lows and the density anomalies in Fig. 8 mark the inferred location of the independent subduction zones: the oldest is the one to the northeast while the subduction beneath the Zagros mountains (to the southwest) is the active one.

Conclusion

Absolute S-wave velocity structures of the lithosphere-asthenosphere system beneath a seismic profile in Iran were defined by simultaneously inverting data from receiver functions and

fundamental mode Rayleigh wave group velocity. The seismic profile crosses the Zagros, Sanandaj-Sirjan Zone (SSZ), Urumieh-Dokhtar magmatic arc (UDMA), Central Iran, Alborz-Binalud mountain ranges and Kopeh Dagh mountain ranges. To validate the resolved S-wave velocity structures, Bouguer anomaly data have been inverted with the geometrical constrain taken from the S-wave velocity models. The main results obtained are listed below:

1. The upper crust thickness varies considerably beneath the profile: it is thinner in the middle part beneath Central Iran. A roughly similar trend is observed for the total crustal thickness, with the exception of two abrupt changes beneath SSZ and UDMA at the south, and beneath Binalud foreland at the north. Thin crust in Central Iran may be explained by the rifting episode along the passive margins of microcontinents that characterized this Tethyan realm (e.g., Sengor and Natalin, 1996).

2. The high velocity lithosphere of the Arabia Plate, plunging beneath Central Iran, is clearly observed beneath Zagros. This feature represents the leading edge of Arabian shield subduction beneath Central Iran. The V-shape low velocity/density anomaly in the upper mantle observed beneath the MZT can be interpreted as an intra-lithospheric layer thickened within the continental collision zone.

3. The two low velocity/density anomalies observable in our model beneath the thin lithosphere of Central Iran (thickness ~ 135 km) can be interpreted as due to partial melting in the mantle wedge above the Arabian slab, and feeding this magmatic arc (located beside UDMA) and feeding the magmatic extrusions observed around Lut block, respectively.

4. The subduction under Zagros apparently interrupts the LVZ, hence weakening and thinning the inferred NE-ward mantle flow, according to the notion of relative westerly directed net rotation of the lithosphere (Panza et al., 2010).

5. The presence of at least two independent ophiolite belts in Iran supports the presence of two separate ocean branches, which allowed the initiation of two NE-directed subduction zones. The southwestern one is the most active and responsible for the present seismicity,

whereas the northern one could be a result of an earlier Mesozoic-Early Cenozoic Cimmeride subduction. The two subduction zones are coherent with the thicker and possibly doubled lithosphere in northeastern and southwestern Iran respectively, with the intervening lithosphere which underwent Mesozoic Tethian rifting (Fig. 9).

Acknowledgements

We warmly thank Esmaeil Shabanian (IASBS) for his helpful and constructive comments and discussion. We warmly thank the observers and drivers who enthusiastically participated in the fieldwork. Especial thank to Daniel Rham (Cambridge University) for his valuable helps during installation of the seismic stations. We appreciate Habib Rahimi (University of Tehran) for supplying dispersion curves. We thank Robert Herrmann who provided the receiver function/surface wave inversion routine. We thank the editor and two anonymous reviewers for their constructive comments. First author has been financially supported by the Abdus Salam International Center for Theoretical Physics (ICTP) through bilateral IIEES-ICTP agreement during 6 months visiting of ICTP SAND group. This research is supported by the International Institute of Earthquake Engineering and Seismology (IIEES) under research project 5339 entitled: study of lateral velocity variation of the upper mantle in Northeast Iran continental collision zone. Seismic instrumentation for the fieldwork described in this research was provided by SEISUK and Cambridge University. This research has benefited also from the partial support from the project 2010-2011, funded by Italian MIUR (Ministero dell'Istruzione, dell'Università e della Ricerca): "Subduction and exhumation of continental lithosphere: implications on orogenic architecture, environment and climate".

References

Afshar Harb, A., 1979. The stratigraphy, tectonics and petroleum geology of the Kopet Dagh region, northeastern Iran, PhD thesis, Petroleum Geology Section, Royal School of Mines, Imperial College of Science and Technology, London.

Alavi, M., 1992. Thrust tectonics of the Binalood region, NE Iran. Tectonics 11, 360–370.

Alavi, M., 1996. Tectonostratigraphic synthesis and structural style of the Alborz mountain system in northern Iran. Journal of Geodynamics 21, 1–33.

Al-Damegh, K., Sandvol, E., Al-Lazki, A., Barazangi, M., 2004. Regional seismic wave propagation (Lg and Sn) and Pn attenuation in the Arabian Plate and surrounding regions, Geophysical Journal International 157, 775–795, doi:10.1111/ j.1365-246X.2004.02246.x.

Alinaghi, A., Koulakov, I., Thybo, H., 2007. Seismic tomographic imaging of P- and S waves velocity perturbations in the upper mantle beneath Iran. Geophysical Journal International 169, 1089–1102.

Al-Lazki, A., Seber, I., D., Sandvol, E., Turkelli, N., Mohamad, R., Barazangi, M., 2003. Tomographic Pn velocity and anisotropy structure beneath the Anatolian plateau (eastern Turkey) and the surrounding regions, Geophysical Research Letters 30, 24, 8043.

Al-Lazki, A.I., Sandvol, E., Seber, D., Barazangi, M., Turkelli, N., Mohamad, R., 2004. Pn tomographic imaging of mantle lid velocity and anisotropy at the junction of the Arabian, Eurasian and African plates. Geophysical Journal International 158, 1024–1040.

Allen, M., Armstrong, H., 2008. Arabia–Eurasia collision and the forcing of mid-Cenozoic global cooling. Palaeogeography, Palaeoclimatology, Palaeoecology 265, 52–58.

Amini S., Shomali, Z.H., Koyi, H., Roberts, R.G., 2012, Tomographic upper-mantle velocity structure beneath the Iranian Plateau, Tectonophysics 554–557, 42-49.

Ammon C. J., G.E. Randall, and G. Zandt (1990): On the nonuniqueness of receiver function inversions, Journal of Geophysical Research 95, 15303-15318.

Bird, P., 1978 Finite-element modeling of lithosphere deformation: The Zagros collision orogeny, Tectonophysics 50, 307-336.

Cuffaro, M., Caputo, M., Doglioni, C., 2008. Plate sub-rotations. Tectonics 27, TC4007, doi:10.1029/2007TC002182, 2008

Carminati, E., Giardina, F., Doglioni, C., 2002: Rheological control of subcrustal seismicity in

the Apennines subduction (Italy). Geophysical Research Letters 29, 18, 1882, doi:10.1029/2001GL014084.

Chen, W.P., Yang, Z., 2004. Earthquakes Beneath the Himalayas and Tibet: Evidence for Strong Lithospheric Mantle. Science 304, 5679 pp. 1949-1952, DOI: 10.1126/science.1097324

Chiu, H.Y., Chung, S.L., Zarrinkoub, M.H., Mohammadi, S.S., Khatib, M.M., Iizuka, Y., 2013, Zircon U–Pb age constraints from Iran on the magmatic evolution related to Neotethyan subduction and Zagros orogeny, Lithos162–163, 70–87.

Crespi, M., Cuffaro, M., Doglioni, C., Giannone, F., and Riguzzi, F., 2007. Space geodesy valida- tion of the global lithospheric flow, Geophysical Journal International 168, 491–506, doi: 10.1111/j.1365-246X.2006.03226.x.

Doglioni, C., Carminati, E., Cuffaro, M., Scrocca, D., 2007: Subduction kinematics and dynamic constraints. Earth Science Reviews 83, 125-175, doi:10.1016/j.earscirev.2007.04.001.

Engdahl, E.R., Jackson, J.A., Myers, S.C., Bergman, E.A., Priestley, K., 2006. Relocation and assessment of seismicity in the Iran region, Geophysical Journal International 167, 761–778.

Foulger G.R., Panza G.F., Artemieva I.M., Bastow I.D., Cammarano F., Evans J.R., Hamilton W.R., Julina B.R., Lustrino M., Thybo H. and Yanovskaya T.B., 2013. Caveats on tomographic images, Terra Nova 25, 259-281. DOI: 10.1111/ter.12041.

Hatzfeld, D., Tatar, M. Priestley, K., Ghafor-Ashtiany, M., 2003, Seismological constraints on the crustal structure beneath the Zagros Mountain belt (Iran), Geophysical Journal International 155, 403–410.

Hatzfeld, D., Molnar. P., 2010. Comparisons of the kinematics and deep structures of the Zagros and Himalaya and of the Iranian and Tibetan plateaus and geodynamic implications, Reviews of Geophysics 48, RG2005.

Herrmann, R.B., Ammon, C.J., 2003. Computer Programs in Seismology, Versoin 3.20, Surface Waves, Receiver funcions and Crustal structure, Department of Earth and Atmospheric Sciences, Saint Louis University, St Louis.

Hessami, K., Koyi, H., Talbot, C., Tabassi, H.,Shabanian, E., 2001. Progressive unconformities within an evolving foreland fold-thrust belt, Zagros Mountains, Journal of the Geological Society 158, 969–981.

Hessami, K., Jamali, F., Tabassi, H., 2003. Major active faults of Iran, edition 2003. International Institute of Earthquake Engineering and Seismology, Tehran

Hollingsworth, J., Jackson, J., Walker, R., Gheitanchi, M.R., Bolourchi, M.J., 2006. Strike-slip faulting, rotation and along-strike elongation in the Kopeh Dagh Mountains, NE Iran. Geophysical Journal International 166, 1161–1177.

Hwang, H.J., Mitchell, B.J., 1986. Inter-station surface wave analysis by frequency-domain Wiener deconvolution and modal isolation, Bulletin of the Seismological Society of America 76, 847-864.

Julia, J., Ammon, C.J., Herrmann, R.B. Correig, A.M., 2000. Joint inversion of receiver function and surface wave dispersion observations, Geophysical Journal International 143, 1–19.

Kadinsky-Cade, K., Barazangi, M., Oliver, J., Isacks, B., 1981. Lateral variations in high-frequency seismic wave propagation at regional distances across the Turkish andIranian plateaus, Journal of Geophysical Research 86, 9377–9396.

Kaviani, A., Paul, A., Bourova, E., Hatzfeld, D., Pedersen, H., Mokhtari, M., 2007. A strong seismic velocity contrast in the shallow mantle across the Zagros collision zone (Iran). Geophysical Journal International 171, 399–410.

Levshin, A.L., Pisarenko, V.F., Pogrebinsky, G.A., 1972. On a frequency time analysis of oscillations. Annales Geophysicae 28, 211–218.

Levshin, A.L., Ratnikova, L., Berger, J., 1992. Peculiarities of surface wave propagation across Central Eurasia, Bulletin of the Seismological Society of America 82, 2464–2493.

Ligorria, J.P., Ammon, C.J. 1999. Iterative deconvolution and receiver-function estimation, Bulletin of the Seismological Society of America 89(5), 1395–1400.

Ludwig, W.J., Nafe, J.E., Drake, C.L., 1970. Seismic refraction, Wiley InterScience, New York.

Lyberis, N., Manby, G., 1999. Oblique to orthogonal convergence across the Turan block in the post-Miocene, American Association of Petroleum Geologists Bulletin 83(7), 1135–1160.

Mazhari, S.A. Safari, M., 2013. High-K calc-alkaline plutonism in Zouzan, NE of Lut block, Eastern Iran: An evidence for arc related magmatism in Cenozoic. Journal of the Geological Society of India 81, 5, 698-708

Maggi, M., Jackson, J., McKenzie, D., Priestley, K., 2000. Earthquake focal depths, effective elastic thickness, and the strength of the continental lithosphere. Geology 28 (6), 495–498.

Maggi, A., Priestley, K., 2005. Surface waveform tomography of the Turkish Iranian plateau.

Geophysical Journal International 160, 1068–1080.

Menke, W., 1989. Geophysical Data Analysis: Discrete Inverse Theory, Academic Press, Inc., New York.

Mitchell, B.J., 1995, Anelastic structure and evolution of the continents from seismic surface wave attenuation, Reviews of Geophysics 33, 441-462.

Mohammadi, E., Sodoudi, F., Kind, R., Rezapour, M., 2013a. Presence of a layered lithosphere beneath the Zagros collision zone, Tectonophysics 608, 366–375.

Mohammadi, N., Sodoudi, F., Mohammadi, E., Sadidkhouy, A., 2013b. New constraints on lithospheric thickness of the Iranian plateau using converted waves, Journal of Seismology 17(3), 883-895.

Molnar, P., Oliver, J., 1969. Lateral variations of attenuation in the uppermost mantle and discontinuities in the lithosphere, Journal of Geophysical Research 74, 2648–2683.

Motaghi, K., Tatar, M., Priestley, K., 2012a. Crustal thickness variation across the northeast Iran continental collision zone from teleseismic converted waves. Journal of Seismology 16, 253–260.

Motaghi, K., Tatar, M., Shomali Z.H., Kaviani, A., Priestley, K., 2012b. High resolution image of uppermost mantle beneath NE Iran continental collision zone, Physics of the Earth and Planetary Interiors 208-209, 38–49.

Mouthereau, F., Lacombe, O., Vergés, J., 2012), Building the Zagros collisional orogen: Timing, strain distribution and the dynamics of Arabia/Eurasia plate convergence, Tectonophysics 532–535, 27–60.

Müller, S., Panza, G.F., 1986. In: Wezel, F.C. (Ed.), Evidence of a Deep-reaching Lithospheric Root under the Alpine Arc. The Origin of Arcs, vol. 21. Elsevier, pp. 93–113.

Pang, K. N., Chung, S. L., Zarrinkoub, M. H., Mohammadi, S. S., Yang, H. M., Chu, C. H., ... & Lo, C. H. 2012. Age, geochemical characteristics and petrogenesis of Late Cenozoic intraplate alkali basalts in the Lut–Sistan region, eastern Iran. Chemical Geology, 306, 40-53.

Panza, G.F., 1981, The resolving power of seismic surface waves with respect to crust and upper mantle structural models. In: The solution of the inverse problem in geophysical interpretation. Cassinis R. edition, Plenum Publishing Corporation 39-77.

Panza, G.F., Müller, S., 1978. The plate boundary between Eurasia and Africa in the Alpine Area. Memorie di Scienze Geologiche (Padova) 33, 43–50.

Panza, G.F.,Müller, S.,Calcagnile,G., Knopoff, L., 1982. Delineation of the north central Italian upper mantle anomaly. Nature 296, 238–239.

Panza, G.F., Doglioni, C. and Levshin, A., 2010. Asymmetric ocean basins, Geology 38, 1, 59-62.

Paul, A., Kaviani, A., Hatzfeld, D., Vergne, J., Mokhtari, M., 2006. Seismological evidence for crustal-scale thrusting in the Zagros Mountain belt (Iran). Geophysical Journal International 166, 227–237.

Paul, A., Kaviani, A., Hatzfeld, D., Tatar, M., Pequegnat, C., 2010. Seismic imaging of the lithospheric structure of the Zagros Mountain belt (Iran). In: Leturmy, P., Robin, C. (Eds.), Tectonic and stratigraphic evolution of Zagros and Makran during the Meso-Cenozoic, Geological Society, London, Special Publications 330, 5–18.

Priestley, K., McKenzie,D., 2006. The thermal structure of the lithosphere from shear wave velocities, Earth and Planetary Science Letters 244, 285–301.

Priestley, K., McKenzie, D., Barron, J., Tatar, M., Debayle, E., 2012. The Zagros core: Deformation of the continental lithospheric mantle, Geochemistry, Geophysics, Geosystems 13, Q11014.

Rahimi, H., Hamzehloo, H., Vaccari, F., Panza, G.F., 2014. Shear-wave velocity tomography of the lithosphere–asthenosphere system beneath the Iranian Plateau, under review in Bulletin of the Seismological Society of America.

Ries, J.C., Bettadpur S., Poole, S., Richter, T., 2011. Mean Background Gravity Fields for GRACE Processing, presented at the GRACE Science Team Meeting, Austin, TX, August 8-10.

Sandvol, E., Al-Damegh, K., Calvert, A., Seber, D., Barazangi, M., Mohamad, R., Gok, R., Turkelli, N., Gurbuz, C., 2001. Tomographic imaging of Lg and Sn propagation in the Middle East, Pure and Applied Geophysics 158, 1121–1163.

Sengor, A.M.C., Natalin, B.A., 1996. Paleotectonics of Asia: fragments of a synthesis. In: The Tectonic Evolution of Asia, A. Yin, M. Harrison (Eds), pp. 486-641

Shabanian, E., Siame, L., Bellier, O., Benedetti, L., Abbassi, M.R., 2009. Quaternary slip rates along the northeastern boundary of the Arabia–Eurasia collision zone (Kopeh Dagh Mountains, Northeast Iran). Geophysical Journal International 178, 1055–1077.

Shad Manaman, N., Shomali, H., Koyi, H., 2011. New constraints on upper-mantle Svelocity structure and crustal thickness of the Iranian plateau using partitioned waveform inversion. Geophysical Journal International 184, 247–267.

Shomali, Z.H., Keshvari, F., Hassanzadeh, J., Mirzaei, N., 2011. Lithospheric structure beneath the Zagros collision zone resolved by non-linear teleseismic tomography Geophysical Journal International 187, 394-406.

Stöcklin, J., 1968. Structural history and tectonics of Iran: A review, American Association of Petroleum Geologists Bulletin 52(7), 1229–1258.

Stöcklin, J. 1974. Possible ancient continental margins in Iran, in The Geology of Continental Margins, edited by C. A. Burke and C. L. Drake, pp. 873–887, Springer, New York.

Stoneley, R., 1981. The geology of the Kuh-e-Dalneshin area of southern Iran, and its bearings on the evolution of southern Thetys, Journal of the Geological Society, London, 138, 509-526.

Tatar, M., Hatzfeld, D., Martinod, J., Walpersdorf, A., Ghafori-Ashtiany, M., Chéry, J., 2002. The present-day deformation of the central Zagros from GPS measurements, Geophysical Research Letters 29(19), 1927.

Tatar, M., Hatzfeld, D., Ghafori-Ashtiany, M., 2004. Tectonics of the Central Zagros (Iran) deduced from microearthquake seismicity, Geophysical Journal International 156, 255–266.

Turkelli, N., et al. (2003), Seismogenic zones in eastern Turkey, Geophysical Research Letters 30(24), 8039.

Urban, L., Cichowicz, A., Vaccari, F., 1993. Computation of analytical partial derivatives of phase and group velocities for Rayleigh waves with respect to structural parameters. Studia Geophysica et Geodaetica 37, 14-36.

Vernant, Ph., Nilforoushan, F., Hatzfeld, D., Abbassi, M.R., Vigny, C., Masson, F., Nankali, H., Martinod, J., Ashtiani, A., Bayer, R., Tavakoli, F., Chéry, J., 2004. Present-day crustal deformation and plate kinematics in the Middle East constrained by GPS measurements in Iran and northern Oman. Geophysical Journal International 157, 381–398.

Walker, R., Gans, P., Allan, M., Jackson, J., Khatib, M., Saunders, A., Zarrinkoub, M., 2009. Late Cenozoic volcanism and rates of active faulting in eastern Iran, Geophysical Journal International 177, 783–805

Yanovskaya, T.B., Ditmar, P.G., 1990. Smoothness criteria in surface-wave tomography, Geophysical Journal International 102, 63-72.

Zhu, L.P., Kanamori, H., 2000. Moho depth variation in southern California from teleseismic receiver functions. Journal of Geophysical Research 105, 2969–2980.

Figure captions

Figure 1: Study area; region covered by seismic stations (triangles: Zagros profile, inverted triangles: NE Iran profile) along a line (A-B) from the Zagros which is the north edge of Arabian Plate in Iran across the Sanandaj Sirjan metamorphic Zone (SSZ), the Urumieh-Dokhtar magmatic arc (UDMA), Central Iran, the Alborz-Binalud Mountains to the Kopeh Dagh Mountains which is the south edge of Eurasian Turan Plate. Solid lines represent the active faults (Hessami et al. 2003). The distance along the profiles is calculated relative to NIK (black triangle) with positive values in the NE direction. Geological map modified from the structural map of NGDIR (National Geoscience Database of Iran, http://www.ngdir.ir). MZT: main Zagros thrust fault, DF: Doruneh fault, ATR: Atrak river.

Figure 2: Azimuthal distribution of 250 events used in this study (circles) in relationship to the study area (triangle).

Figure 3: Final results obtained for the four different parameterizations performed for the station KAM (shown in Fig. 1). The starting thickness of the layers was determined by Rahimi et al., (2014) using the concept of the resolving power of dispersion data (Panza 1981). The thickness of inverted layers were subdivided in sub-layers with thickness equal to the IS divided by 1 (a), 1.25 (b), 1.5 (c) and 2 (d) respectively. For each case, the percentage indicates the average value obtained for the fit (between theoretical and experimental RFs) considering all the initial models.

Figure 4: Simplifying the inverted velocity model for station CHA (shown in Fig. 1). a) Observed stacked receiver function (black line) with its error bar (black dashed lines) and synthetic (red line) receiver function computed for the simplified crustal model shown by the red line in (c). b) The observed (solid black line) group velocity with its error bar (black dashed lines) and synthetic (red line) group velocity computed for the simplified crustal model shown by the red line in (c). c) Velocity model obtained from joint inversion (solid blue line) and the simplified crustal model (solid red line), which is considered as the final model. Dashed line is the initial velocity model.

Figure 5: Resolution kernels (red curves) calculated for the chosen parameterization of the final velocity model for station CHA (blue curve, taken from Figure 4.c); the layer number, corresponding to each resolution kernel, is given below the right pane. The kernel plots are

normalized respect to the maximum value of the resolution matrix, whose diagonal elements are related to the resolving power, accordingly with Panza (1981).

Figure 6: 2-D absolute S-velocity structure obtained for the crust beneath seismic profile shown in Fig. 1. The velocity distribution is made from combining of the 1-D models up to the depth of 70 km. Dashed line show crust thickness along profile obtained from the connecting calculated thicknesses for Moho boundary beneath each station (black squares). Inverted triangles show the abscissa of the projection of the stations onto line A-B (Fig. 1). Elevation variations along the profile are also shown on the top of the panel. Abbreviations are the same as in Fig. 1. Bl: Binalud mountain range, KD: Kopeh Dagh mountain range.

Figure 7: the lithosphere-asthenosphere system beneath seismic profile shown in Fig. 1. White circles denote seismicity (Mw>4) for the period 1964–2006 (Engdahl et al. 2006). White squares show the lithosphere thickness extracted from 1-D velocity models. Inverted triangles show the abscissa of the projection of the stations onto line A-B (Fig. 1). Elevation variations along the profile are also shown on the top of the panel. Abbreviations are described in Figs. 1 and 5.

Figure 8: Up: observed Bouguer anomaly (gray squares) along study area as well as predicted Bouguer anomaly (red circles). Down: calculated density distribution with depth (down) along the study area). Elevation variations along the profile are also shown on the top of the density model. Abbreviations are described in Figs. 1 and 5.

Figure 9: Simplified sketch illustrating how Iran could be interpreted as the coalescence of at least two separate subduction zones, the northeastern one the oldest (Cimmerides), and the southwestern slab the second presently active. Volcanism was supplied by magmatism generated by fluids triggering partial melting in the mantle wedge of the upper plate. Since the orogen expanded to the southwest, also the slab and the related magmatism moved in the same direction. L, lower plate, H, subduction hinge, U, upper plate. The black crust is an oceanic embayment or ophiolitic suites in the Cimmerides and later in Zagros. This interpretation is well supported by geological data and the geophysical data (gravity and seismology) discussed in this paper and shown in fig 6, 7 and 8.

Table captions

Table 1: The thickness of the crust and the lithosphere extracted from 1-D velocity models. Stations are ordered based on their position in profile from south to north.

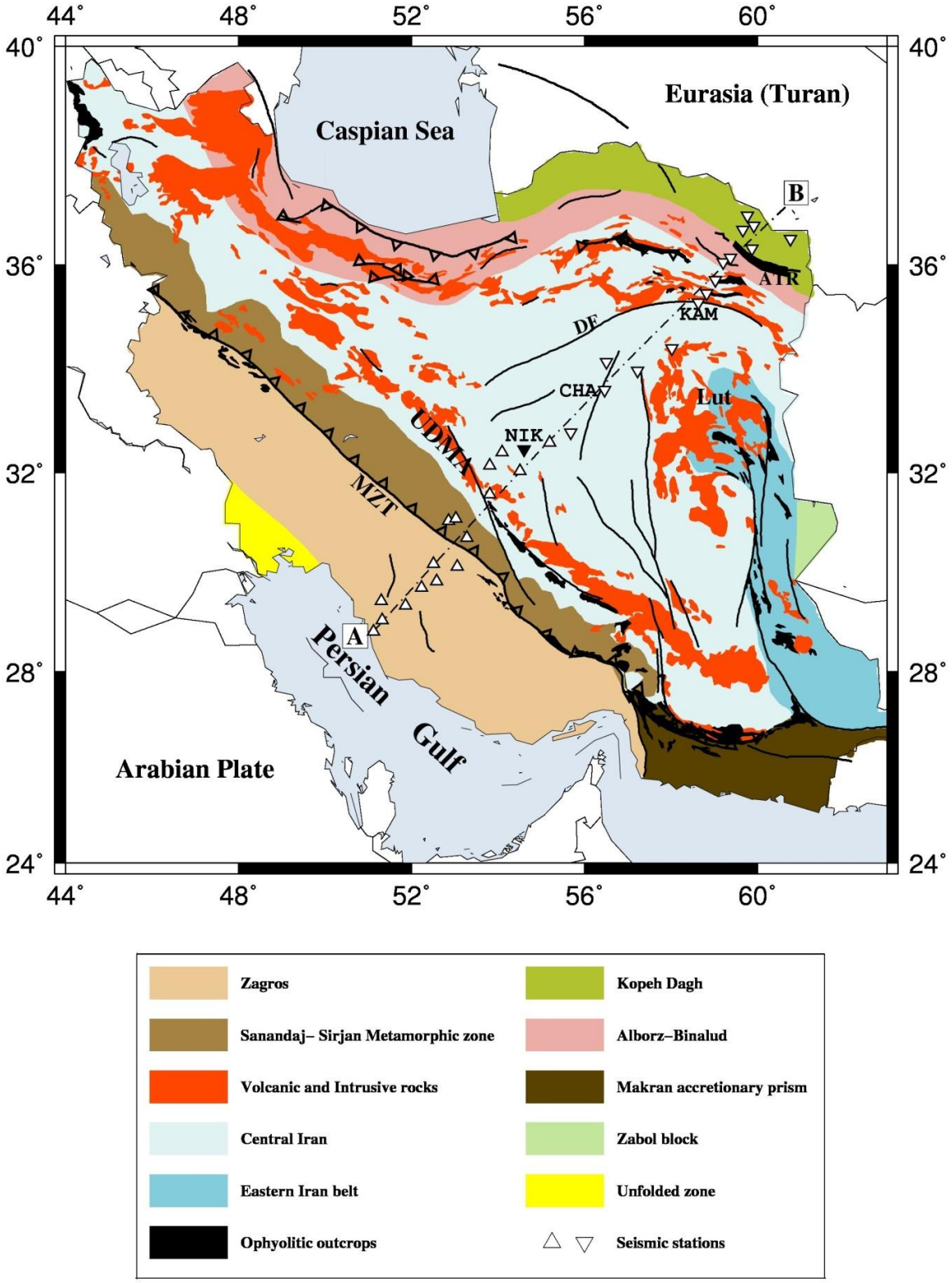

Figure 1

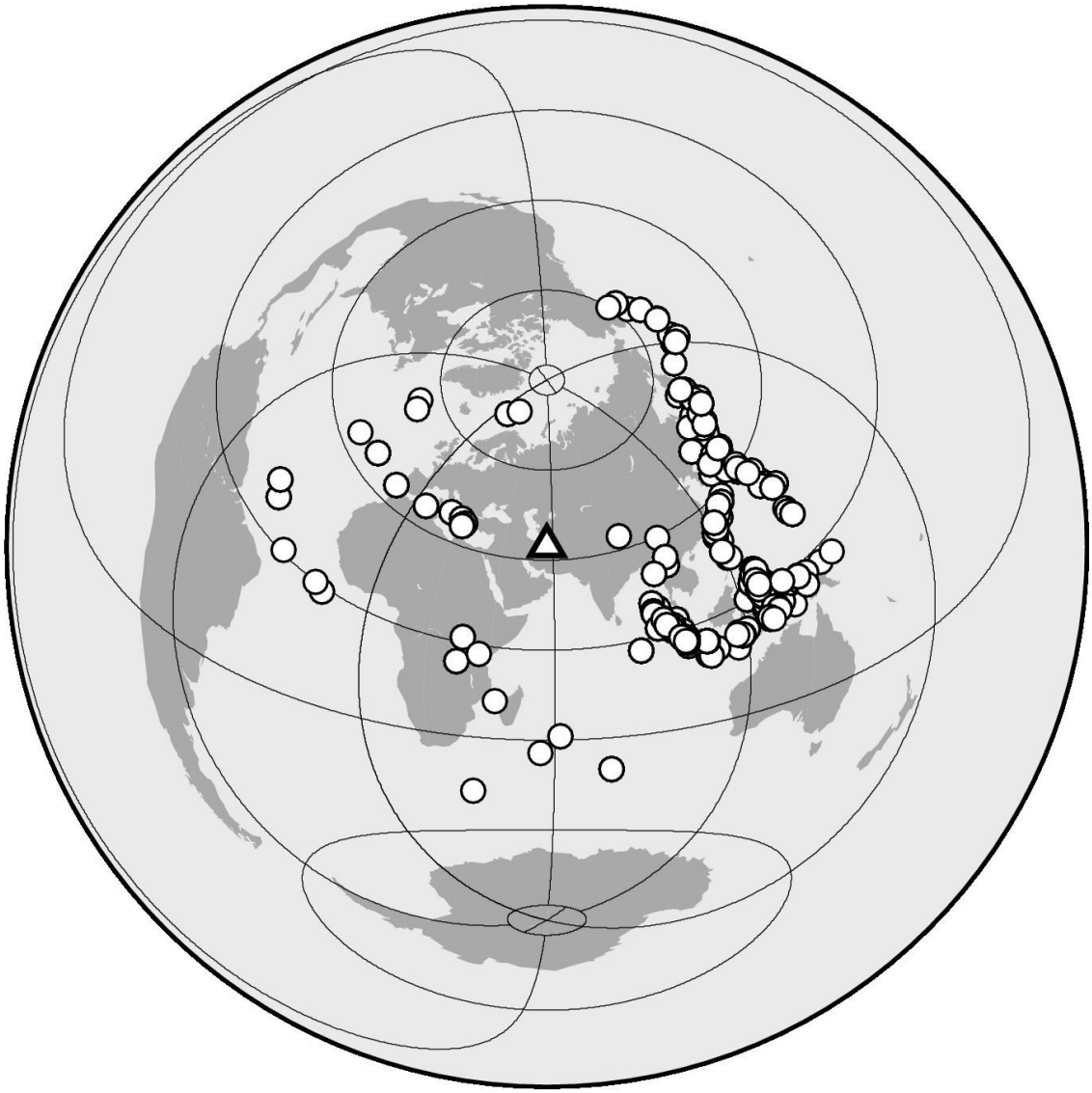

Figure 2

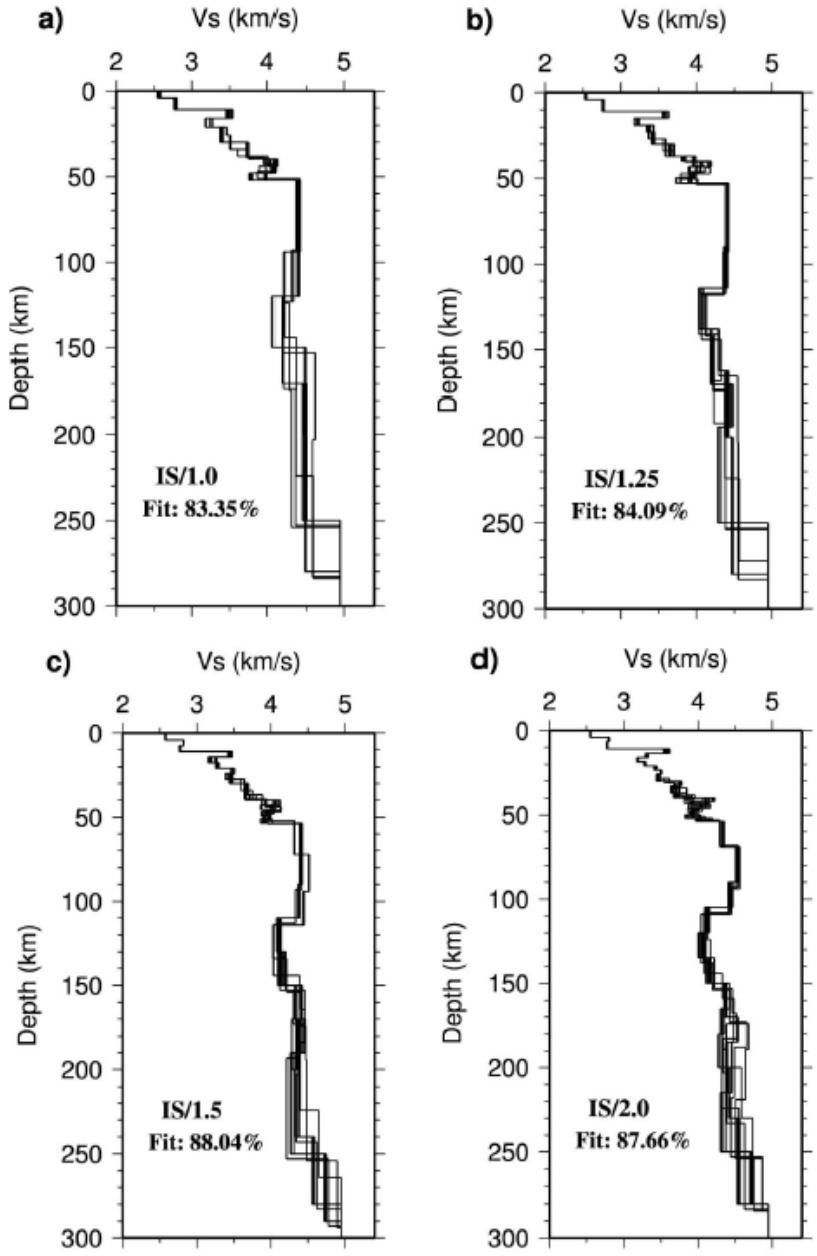

Figure 3

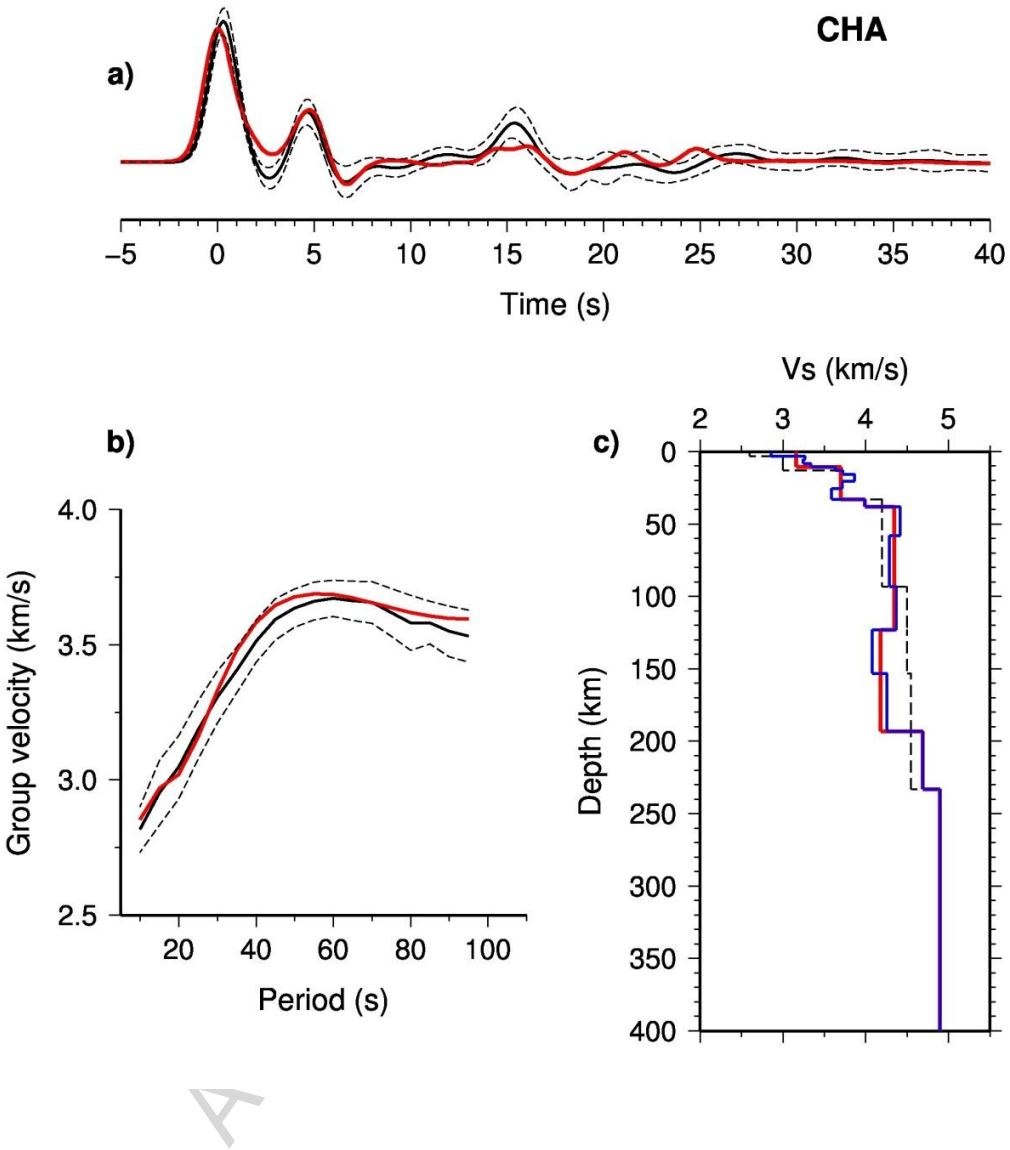

Figure 4

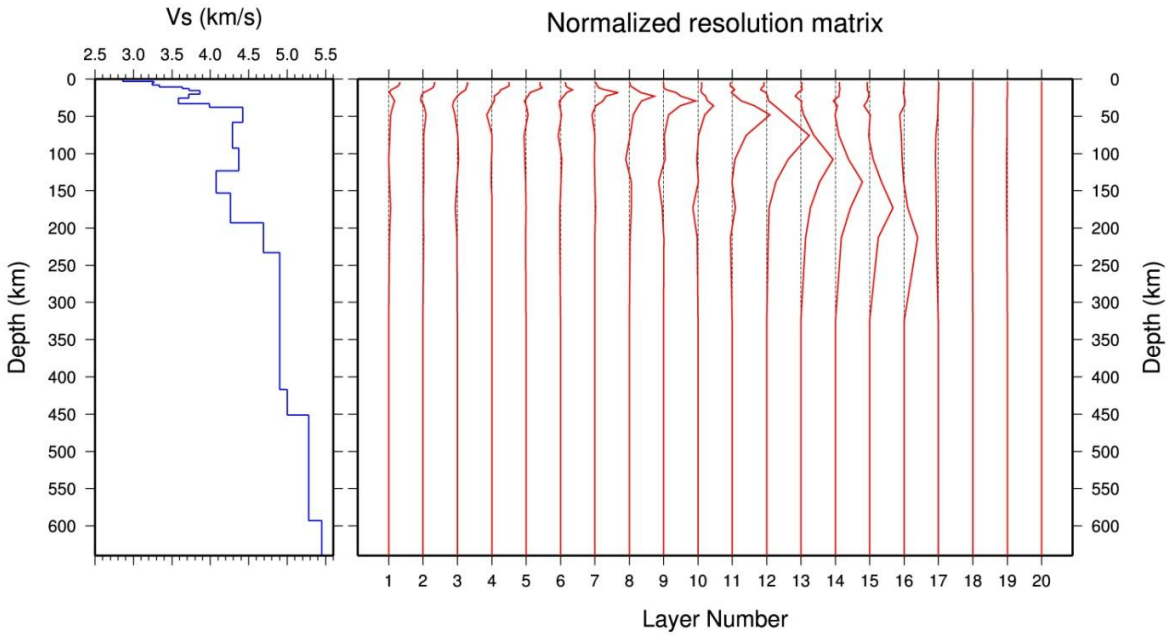

Figure 5

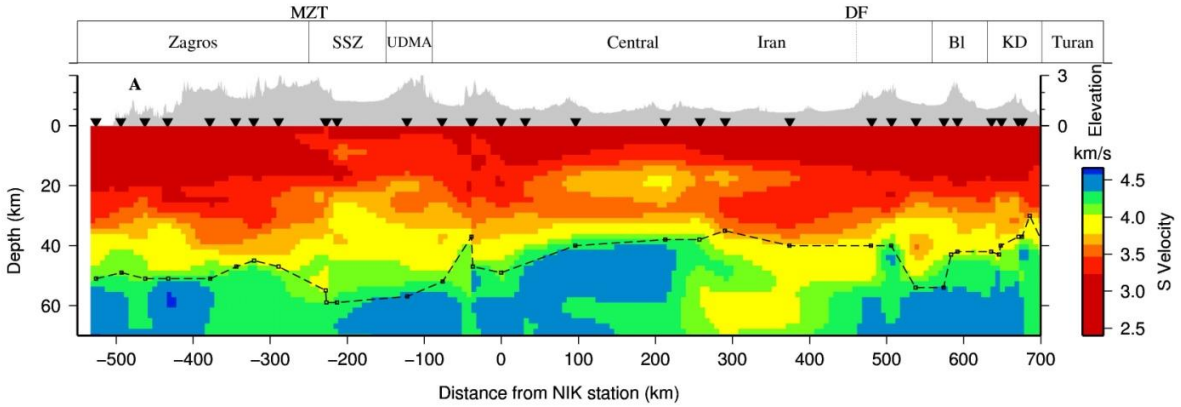

Figure 6

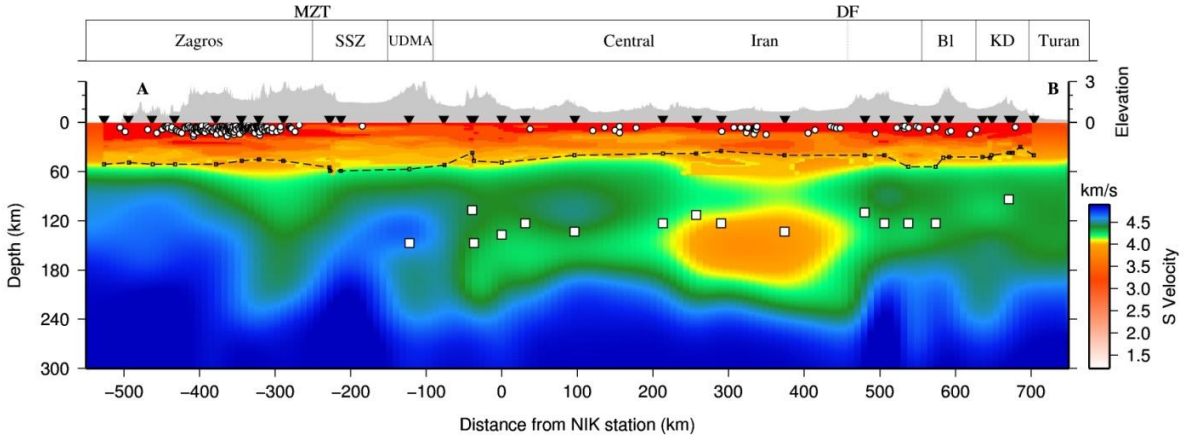

Figure 7

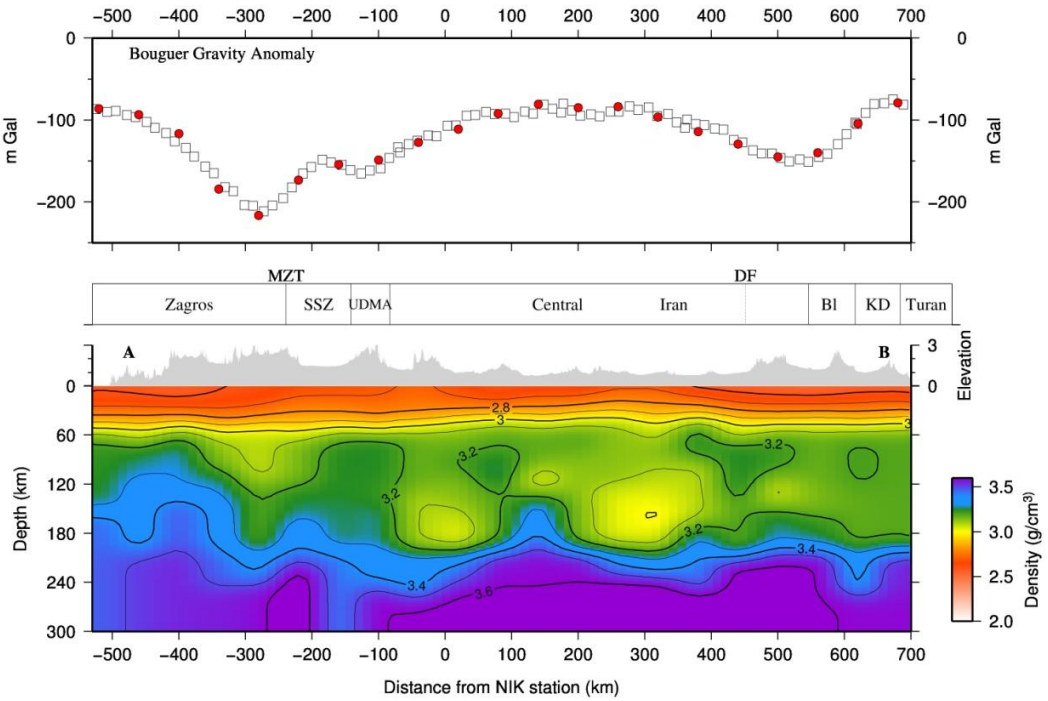

Figure 8

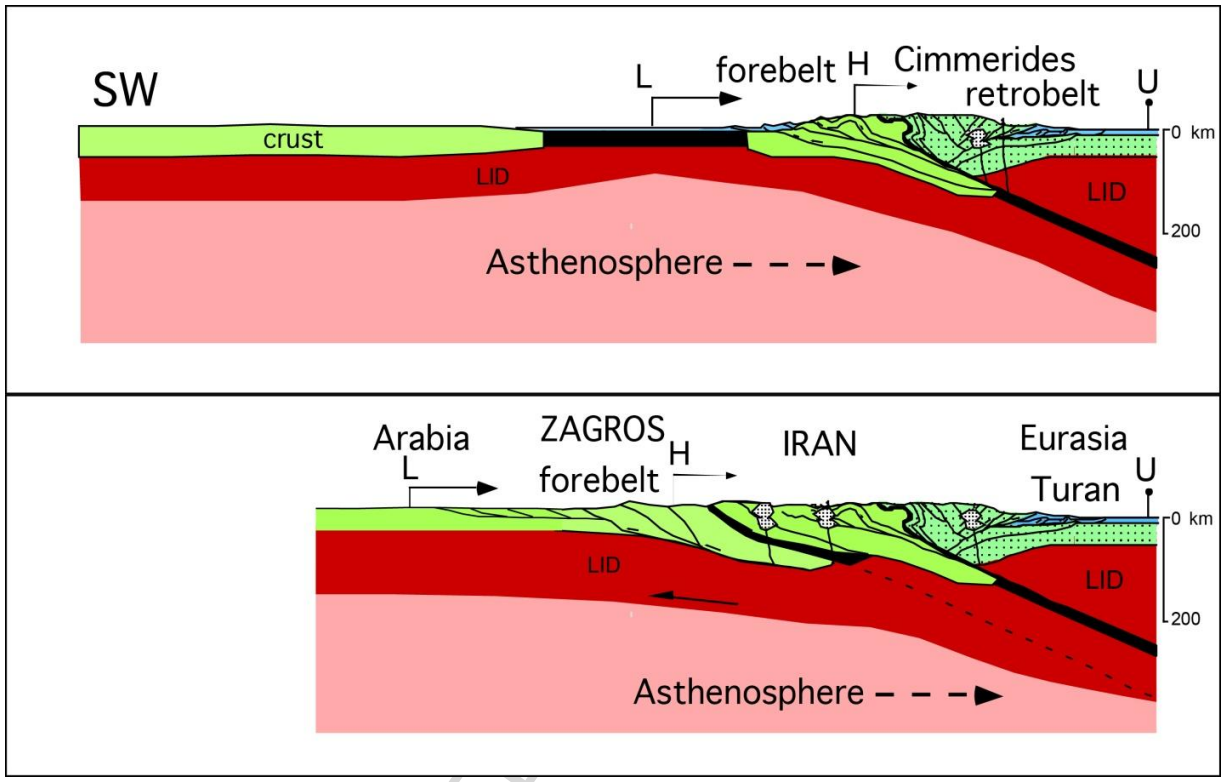

Figure 9

Table 1

Station name	**F13**	**M1**	**A1**	**A3**	**M2**	**B1**	**B2**	**B3**	**M4**
Moho depth	51±1.5	49±1.5	51±2	51±2	51±1.5	47±2	45±2	47±2	59±1.5
LAB depth	-	-	-	-	-	-	-	-	-
Station name	**M5**	**M6**	**C2**	**D1**	**D3**	**NIK**	**M7**	**JAN**	**CHA**
Moho depth	55±1.5	57±1.5	52±1.5	37±1.5	47±1.5	49±3.5	-	40±3.5	38±2.5
LAB depth	-	147	-	107	147	137	123	133	123
Station name	**SAL**	**TAR**	**SEN**	**KAM**	**NAM**	**KTH**	**BAH group 1**	**BAH group 2**	**MOG**
Moho depth	38±2.5	35±2.5	40±3.5	54±1.5	40±1.5	54±1.5	54±1.5	43±1.5	42±1.5
LAB depth	113	123	133	110	123	123	123	-	-
Station name	**KBD group 1**	**KBD group 2**	**KAR**	**ZOW**	**HAM group 1**	**HAM group 2**	**ISG**		
Moho depth	42±1.5	47±2.5	40±1.5	37±1.5	37±1.5	30±1.5	40±2.0		
LAB depth	-	93	-	94	-	120	-		

group 1: model has found using the receiver functions stacked from the back-azimuth: 105^{o}-165^{o} : these back-azimuths differ by less than 30^{o} from the line orthogonal with the east of strike of the array.
group 2- model has found using the receiver functions stacked from the back-azimuth 15^{o}-75^{o}: these back-azimuths differ by less than 30^{o} from the north of strike of the array.

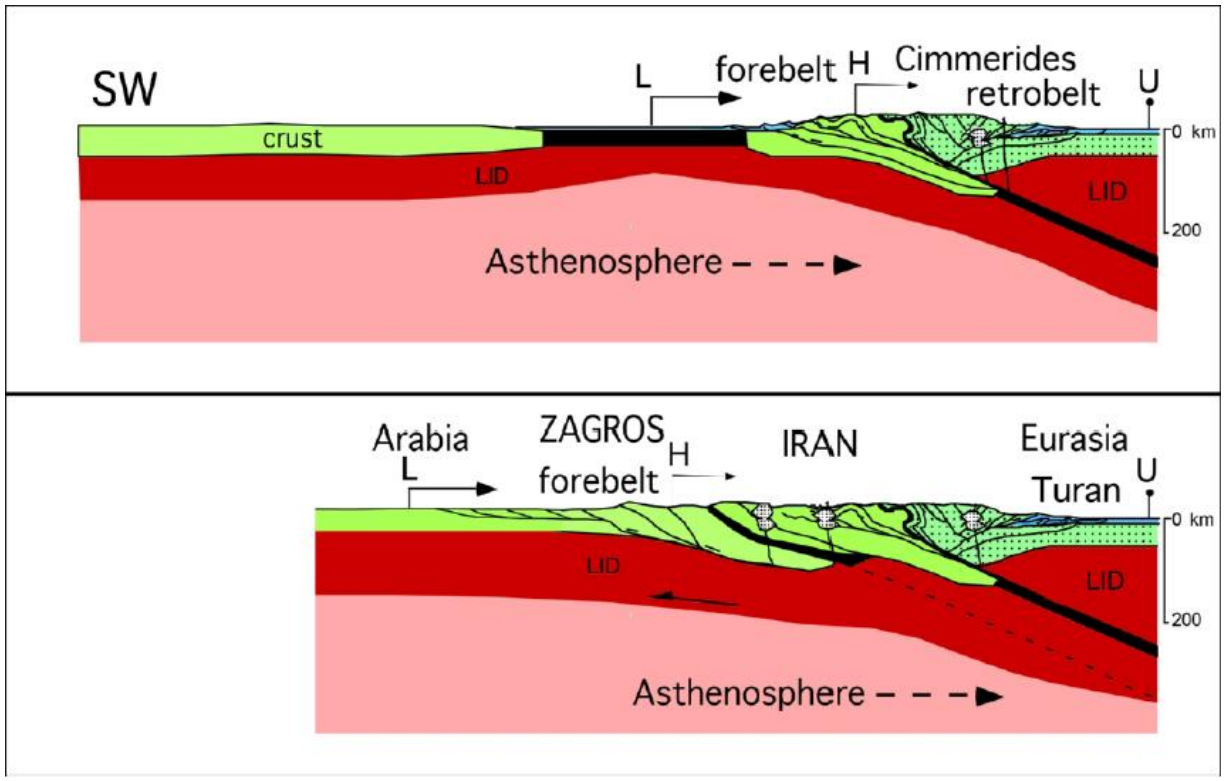

Graphical abstract

Highlights

- High resolution deep structures beneath a seismic profile in Iran are defined.
- The results confirm the presence of crustal roots at the north and south of Iranian Plateau.
- The lithosphere of the Arabian Plate gently plunges NNE-ward beneath Central Iran.
- The results support the double subduction evolution recorded in the surface geology.